Monte Carlo simulation of Raman light scattering in a human skin

I. Matveeva[1], O. Myakinin[1], Y. Khristoforova[1]

[1]Samara National Research University, Moskovskoe Shosse 34, Samara, Russia, 443086

Abstract. The paper presents an algorithm for simulating Raman light scattering inside a human skin using the Monte Carlo method. The proposed algorithm uses the photon transport algorithm developed by L. Wang and S. Jacques as a basis and permits to model heterogeneities of various sizes and topologies caused by pathological processes. A skin optical model has been built with optical transport parameters compiled from Meglinski et al., Jacques and Raman active components of skin cancer from Xu Feng et al. As the most important model components collagen, elastin, keratin, cell nucleus, triolein, ceramide, melanin and water are chosen. Raman spectra of normal human skin, malignant melanoma and basal cell carcinoma skin cancers have been simulated. The reconstructed Raman spectra reached reasonably good match with the skin spectra measured *in vivo*. The possibility of using the algorithm to estimate changes in the concentration of skin components with the development of malignant neoplasm by modeling Raman spectra of normal skin and skin with the malignant neoplasm and comparing them with the corresponding experimental Raman spectra is examined.

1. Introduction

A high increase in the number of detected skin tumours in the Russian Federation (in particular in the Samara region [1]), makes us looking for diagnostic methods that can provide high accuracy in determining the type of newly formed tissue, provide information about its composition, size and topology. The ability to conduct *in vivo* tests, portability, non-invasiveness and accuracy make Raman spectroscopy a leader among modern methods of analysis of skin lesions [2]. A Raman spectrum is formed as a result of the absorption and scattering of radiation by a variety of structures of the biological tissue. During the development of the disease, a change in the biochemical composition of the tissue occurs, which leads to a change in the Raman spectra. Thus, it is possible to evaluate the component composition of the tissue. Therefore, it is important to have a model to illustrate Raman scattering.

2. Methodology

2.1. Skin model

We used a two-layer model of the skin: the epidermis of 0.2 mm and the dermis of 4.8 mm (figure 1). Each voxel of the model is described by the absorption coefficient, scattering coefficient, anisotropy factor and refractive index [3, 4], as well as the concentration of components that form inhomogeneities in the tissue: collagen, elastin, keratin, cell nuclei, triolein, ceramide, melanin, and water (table 1) [5].

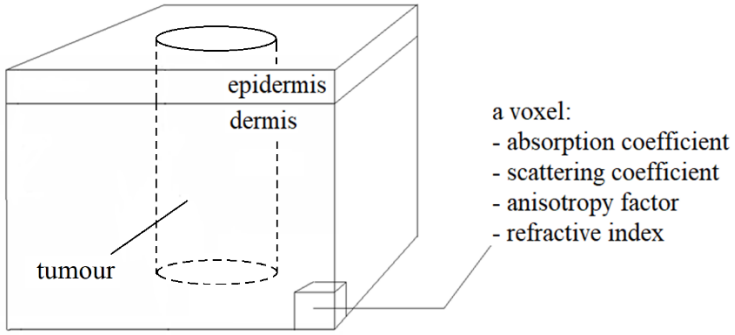

Figure 1. Skin model.

Table 1. Skin components in percentage for different tissue types (the arrow indicates the most significant changes for each lesion type) [5].

	Normal skin	Malignant Melanoma	Basal Cell Carcinoma
Collagen	18%	18%	15%↓
Elastin	12%	14%	23%↑
Triolein	41%	11%↓	28%↓
Nucleus	9%	6%	20%↑
Keratin	1%	2%	1%
Ceramide	9%	17%↑	4%
Melanin	5%	29%↑	3%
Water	5%	3%	6%

Malignant melanoma is modelled as a part of the skin (as a cylinder) with a melanin concentration different from its concentration in normal skin, namely 30%. Clark's classification of the stages of malignant melanoma is used.

A feature of the way in which neoplasms are modelled is that the experimental Raman spectrum of normal skin, obtained by averaging *in vivo* Raman spectra of normal skin, serves as a substrate for the simulated Raman spectrum. The pathology is simulated by adding to the model Raman active components.

2.2. Experimental data

As the Raman spectra of normal skin and skin with a disease we take the averaged Raman spectra of several patients (from 10 to 30 depending on the type of neoplasm). Raman spectra are recorded using a portable setup [6]. All *in vivo* studies were conducted on patients older than 18 years of age and with their consent. The studies were approved by the ethics committee of Samara State Medical University.

2.3. Monte Carlo algorithm for modelling of Raman light scattering

The algorithm consists of the main program and the photon transport subprogram developed on the basis of the algorithm proposed by L. Wang and S. L. Jacques [7]. The description of the developed algorithm is presented in [8]. In the first step, the program simulates the propagation of the incident photons through the sample, which results in a distribution of the excitation photons, *Fex (x, y, z)* within the sample. In the second step, Raman scattered photons are launched from each point where parent photons were absorbed in isotropically distributed directions. During the second step, the program is executed sequentially at each wavelength and the sum of all the photons captured by the detector is calculated. A feature of the developed algorithm is a method for setting the initial weight of the photon packet W_R, which allows to take into account the spatial structure of Raman scattering:

$$W_R(x,y,z,\lambda) = F_{ex}(x,y,z) \times \mu_R(\lambda) \times \left(s_{R1}(\lambda)C_1(x,y,z) + \cdots + s_{RN}(\lambda)C_N(x,y,z)\right), \quad (1)$$

$F_{ex}(x, y, z)$ represents results in a distribution of the excitation photons, $\mu_R(\lambda)$ is comparable with the Raman probability and depends on the frequency of the emission photons, $s_{R1}(\lambda) \dots s_{RN}(\lambda)$ are given by Raman spectra of skin components, $C_1(x, y, z) \dots C_N(x, y, z)$ are concentrations of components.
In formula 1, $\mu_{Raman}(\lambda)$ is determined as:

$$\mu_{Raman}(\lambda) = 1/\lambda^4. \quad (2)$$

3. Results and Discussion

3.1. Monte Carlo simulation of normal skin, Malignant Melanoma, and Basal Cell Carcinoma Raman spectra

Monte Carlo simulation were performed to record Raman spectra of skin for 785 nm excitation light and for different emission wavelengths at am interval of 1 nm from 840 nm to 910 nm. We obtained Raman spectra spanning normal skin, Malignant Melanoma (MM), and Basal Cell Carcinoma (BCC). The concentrations of the most relevant skin constitutes contributing to the spectral differences among different skin malignancies are taken from Feng X. et al. [5] (table 1).

Figure 2 shows mean Raman *in vivo* spectra (blue stipple lines) and reconstructed Raman spectra (red solid lines). The Raman spectra were normalized to their respective area under curve.

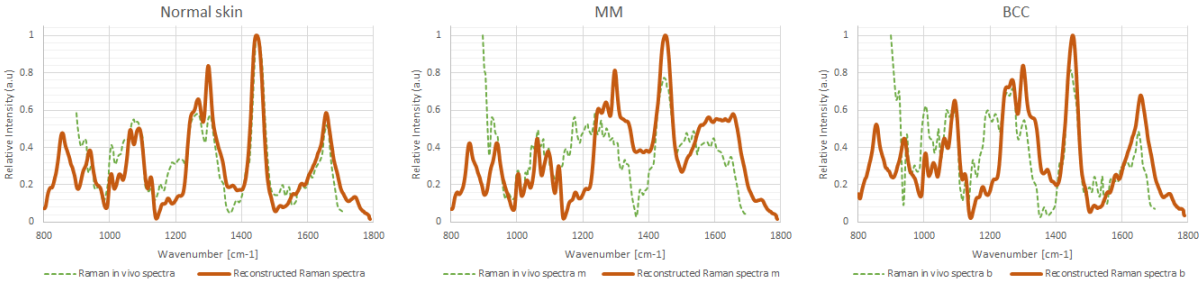

Figure 2. Normalized Raman spectra of normal skin tissue, Malignant Melanoma (MM), and Basal Cell Carcinoma (BCC).

In general, the reconstructed Raman spectra match reasonably well with the *in vivo* Raman spectra. In particular, the major Raman peaks of normal skin Raman spectra reconstructed by this Monte Carlo simulation match very well with the *in vivo* spectra. There are also differences between the reconstructed and the *in vivo* Raman spectra in the case of MM and BCC. These differences may be due to the fact that the composition of diseased skin varies depending on the stage of the disease and individual characteristics of patients.

3.2. Monte Carlo simulation of MM of various stages

Monte Carlo simulation has been performed to record Raman spectra of skin for different emission wavelengths with an interval of 1 nm from 1200 nm to 1800 nm. The MM is simulated by adding to the experimental Raman spectrum of normal skin Raman active melanin. The tumor appears as a cylinder (figure 1). It is assumed that there are two components in the skin model: healthy skin (distributed throughout the volume) and melanin (inside the cylinder).

As a result, Raman spectra of human skin with malignant melanoma of various thickness were obtained (figure 3, d). With an increase in tumour thickness h, the Raman spectrum of human skin changes predominantly in those ranges where the melanin spectrum (figure 3, a) has large intensity values (from 1325 to 1425 1/cm and from 1500 to 1650 1/cm). Experimental spectra with tumour development also demonstrate an increase in intensity in these ranges (figure 3, b). In the case of experimental spectra, changes can be seen in other ranges. The absence of such changes in the reconstructed spectra is explained by the simplicity of the model: during the melanoma development, changes in the skin composition are not limited to melanin, but affect such components as triolein and ceramide [5]. The study of its influence on the Raman spectrum is interesting. The dependence of the Raman spectrum intensity on the tumour thickness looks like exponential (figure 3, c).

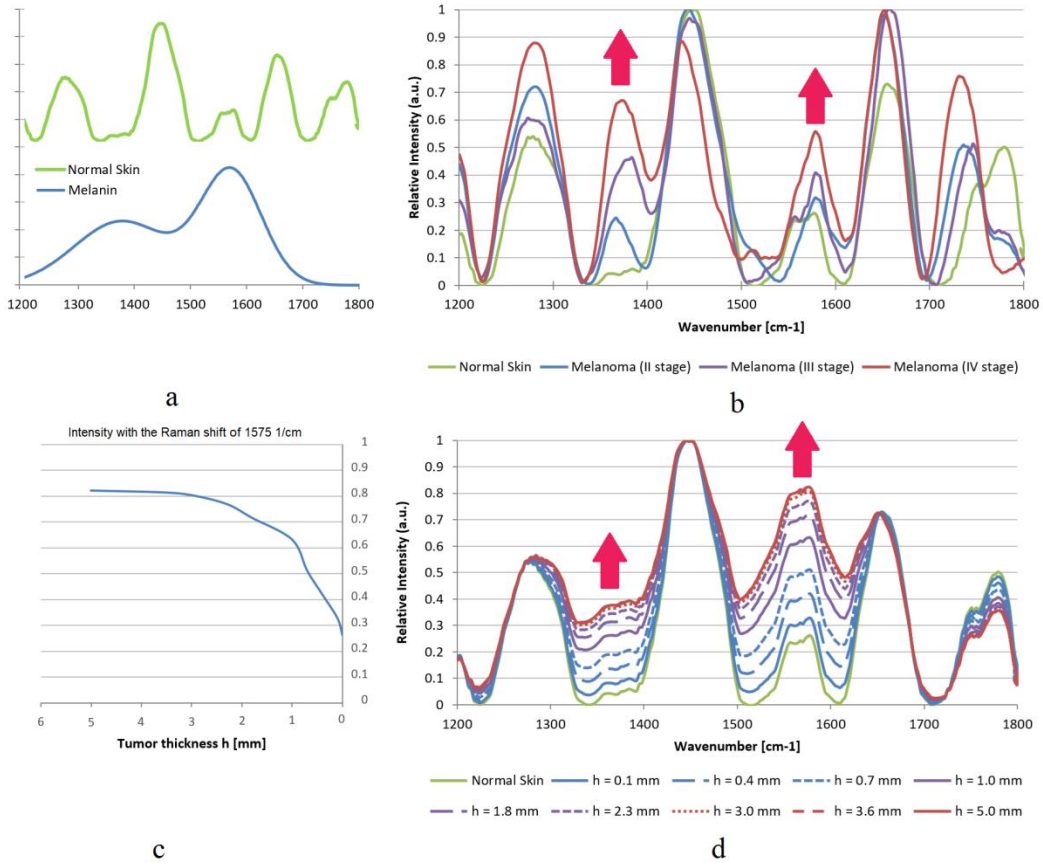

Figure 3. a) Schematic Raman spectra of normal skin and melanin; b) Averaged experimental Raman spectra of human skin; c) Dependence of the Raman spectrum intensity with the Raman shift of 1575 1/cm on the tumor thickness; d) Reconstructed Raman spectra of human skin tissue.

3.3. Determination of changes in the concentrations of skin components during the development of MM and BCC

The skin Raman spectra of several patients, registered *in vivo* were selected for study [5]. For each patient, the normal skin Raman spectra and the MM/BCC Raman spectra are known. The averaged experimental Raman spectrum of normal skin, obtained by averaging normal skin *in vivo* spectra of all the patients, is selected as the «background» spectrum. By varying the concentrations of collagen, elastin, keratin, cell nucleus, triolein, ceramide, melanin and water, it is proposed to obtain a spectrum that is closest to the average experimental MM/BCC Raman spectrum. Figure 4 and figure 5 show the results of simulating the BCC Raman spectrum and the MM Raman spectrum, respectively. The parameters at which the obtained spectrum is closest to the average experimental MM/BCC Raman spectrum are presented in table 2.

Comparing the reconstructed BCC Raman spectrum with the averaged experimental BCC Raman spectrum (figure 4), it can be noted that these spectra are fairly well correlated with each other, especially in the range from 1316 to 1723 1/cm. In the range from 1723 to 1799 1/cm, the resulting Raman spectrum is more similar to the normal skin Raman spectrum, and not to the BCC Raman spectrum. Paying attention to the Raman spectra of skin components (figure 4), it can be noted that in the specified range the spectra of the components have no characteristic peaks. This means that during the development of BCC, changes in the composition of the skin are not limited to the components studied, the change in the experimental spectra in the specified range is due to other components.

Analysing changes in the concentrations of the skin components, one can identify the following. In the transition from the average Raman spectrum of normal skin to the average Raman spectrum of the BCC, the concentrations of collagen, triolein, ceramide, and melanin decrease, and the concentration

of water increases, as also reported in [5]. In the case of elastin, keratin and nucleus, there is a difference in the concentrations from those given in [5].

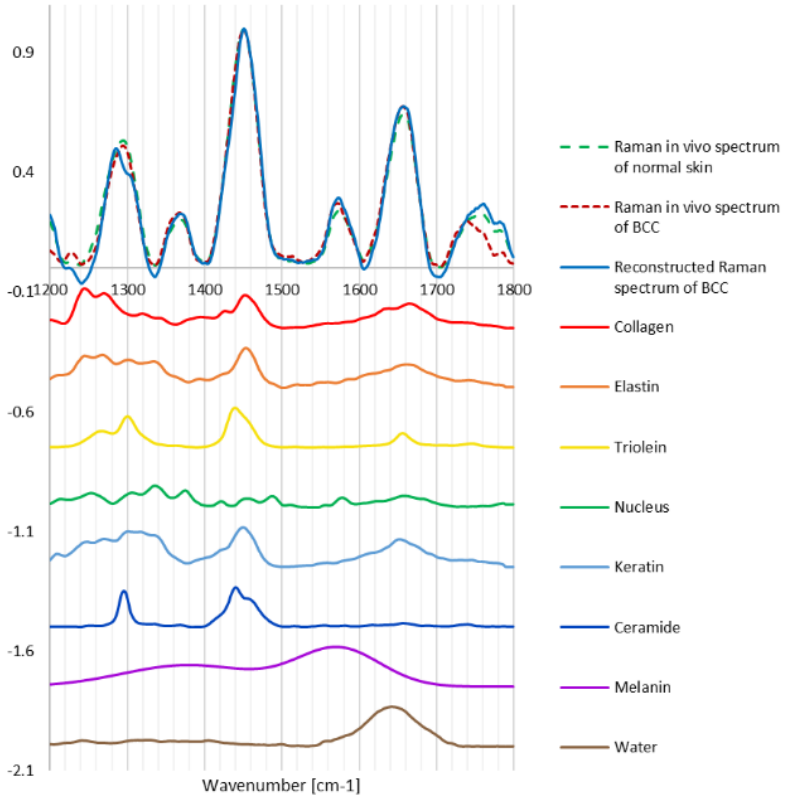

Figure 4. Raman spectra of normal skin, BCC, and some skin components.

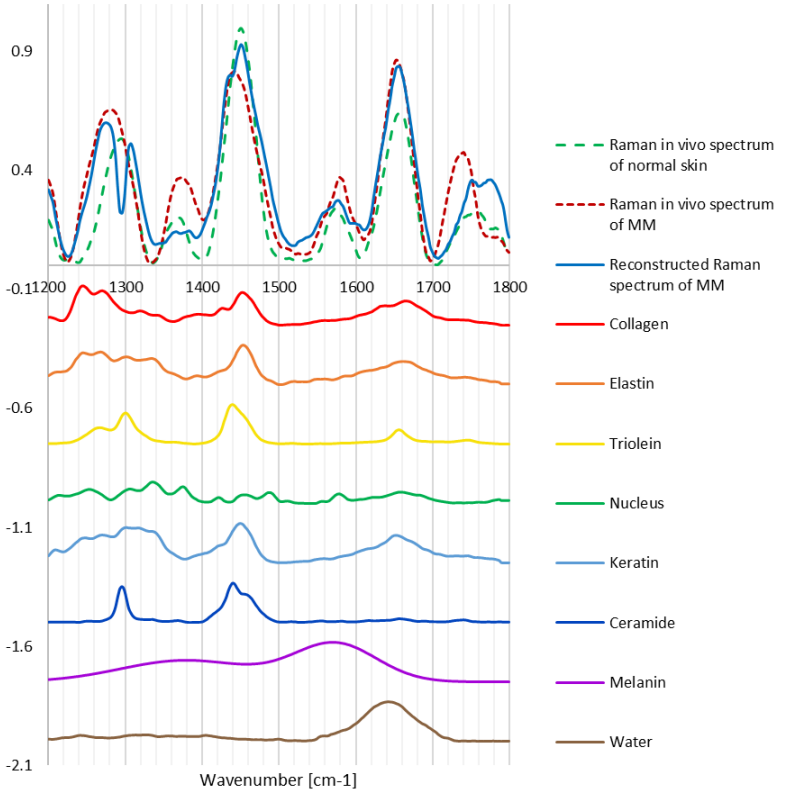

Figure 5. Raman spectra of normal skin, MM, and some skin components.

Thus, in accordance with [5], the concentrations of elastin and nucleus increase by 11%, and the concentration of keratin does not change (table 2). However, as a result of modelling, the concentration of elastin decreases, the concentration of nucleus does not change, and the concentration

of keratin increases. These results may be due to the fact that the composition of BCC varies depending on individual characteristics of patients.

Table 2. Changes in the concentrations of skin components during the transition from the normal skin Raman spectrum to the MM/BCC Raman spectrum.

	Malignant Melanoma (MM)		Basal Cell Carcinoma (BCC)	
	Change in the concentration of the component (by Feng X. et al.)	Change in the concentration of the component (in this study)	Change in the concentration of the component (by Feng X. et al.)	Change in the concentration of the component (in this study)
Collagen	0%	+13%	-3%	-1%
Elastin	+2%	-4%	+11%	-6%
Triolein	-30%	+56%	-13%	-10%
Nucleus	-3%	+17%	+11%	0%
Keratin	+1%	-20%	0%	+4%
Ceramide	+8%	-62%	-5%	-7%
Melanin	+24%	+8%	-2%	-2%
Water	-2%	+2%	+1%	+1%

Comparing the reconstructed MM Raman spectrum with the average experimental MM Raman spectrum (figure 5), it can be noted that these spectra are fairly well correlated with each other, especially in the range from 1200 to 1265, from 1400 to 1440, from 1480 to 1560, from 1600 to 1700 1/cm . In the range from 1440 to 1460, from 1700 to 1740 1/cm, the obtained Raman spectrum is more similar to the Raman spectrum of normal skin. In the range from 1280 to 1300, from 1740 to 1800 1/cm, the obtained spectrum does not coincide with any of the experimental spectra. This means that during the development of MM, changes in the composition of the skin are not limited to the components studied.

In the transition from the average Raman spectrum of normal skin to the average Raman spectrum of the MM, the concentrations of elastin, keratin, and ceramide decrease, and the concentration of collagen, triolein, nucleus, melanin, and water increases (table 2), that are little correlated with [5]. These results may be due to the fact that the composition of MM varies depending on individual characteristics of patients. The main indicator of the development of MM is an increase in the concentration of melanin, as reported in [5]. As a result of the simulation, we also observe similar changes. The effect of the development of malignant melanoma on the concentrations of other components requires additional research.

In summary, spectra modelled were found to be consistent in general with previous studies. The algorithm can be used not only to simulate the Raman spectra but also to study the real Raman spectra of patients and determine certain parameters of these spectra. Monte Carlo simulations of photon propagation offer a flexible yet rigorous approach toward Raman scattering in turbid tissues.

4. Acknowledgments

This study was supported by the RFBR Grant № 19-52-18001 Bolg_a and the Russian Federation President grant for state support of young scientists (project MK-1888.2019.2).

5. References

[1] Kozlov, S.V. Features of the incidence of skin melanoma in the Samara region / S.V. Kozlov, E.Y. Neretin // Yevraziyskiy onkologicheskiy zhurnal. – 2014. – Vol. 1. – P. 114.

[2] Khristoforova, Y.A. Optical diagnostics of malignant and benign skin neoplasms / Y.A. Khristoforova, I.A. Bratchenko, D.N. Artemyev // Procedia Engineering. – 2017. – Vol. 201. – P. 141-147.
[3] Meglinski, I. Dermal component-based optical modeling of skin translucency: impact on skin color / I. Meglinski, A. Doronin, A.N. Bashkatov // Computational Biosphysics of the Skin. – 2014. – P. 25-62.
[4] Jacques, S.L. Optical properties of biological tissues: a review // Physics in Medicine & Biology. – 2013. – Vol. 58(11). – P. R37.
[5] Feng, X. Raman active components of skin cancer / X. Feng, A.J. Moy, H.T. Nguyen // Biomedical Optics Express. – 2017. – Vol. 8(6). – P. 2835-2850.
[6] Khristoforova, Y.A. Portable spectroscopic system for in vivo skin neoplasms diagnostics by Raman and autofluorescence analysis / Y.A. Khristoforova, I.A. Bratchenko, O.O. Myakinin // Journal of Biophotonics. – 2019. – Vol. 12(4). – P. e201800400.
[7] Wang, L. Monte Carlo modeling of light transport in multi-layered tissues in standard C / L. Wang, S.L. Jacques // The University of Texas, MD Anderson Cancer Center, Houston, 1992. – P. 4-11.
[8] Matveeva, I. Monte Carlo modelling of normal skin and skin cancer Raman spectra / I. Matveeva, O. Myakinin // Journal of Physics: Conference Series. – 2019. – Vol. 1368(4). – P. 042084.